

Mechanical Modelling and Stress-Strain Prediction of Electroactive Polymer-Based Capacitive Sensor under Multiaxial Loads using Uniaxial Tensile Data

Nitin Kumar SINGH, Kazuto TAKASHIMA and Shyam S. PANDEY

Graduate School of Life Science and Systems Engineering, Kyushu Institute of Technology,
2-4 Hibikino, Wakamatsu campus, Kitakyushu, Fukuoka 808-0196, Japan,
Telefax: +81-93-695-6230

E-mail: nitinmjpruiitp@gmail.com, singh.nitin-kumar228@mail.kyutech.jp,
nitin.mt12@iitp.ac.in, shyam@life.kyutech.ac.jp

Received: 1 July 2022 /Accepted: 1 August 2022 /Published: 31 October 2022

Abstract: In this paper, mechanical modelling and stress-strain prediction of the ionic type of electroactive polymer (EAP) based capacitive strain sensor under multiaxial loading has been performed using uniaxial tensile data. A highly stretchable sensor with > 400 % strain was fabricated using Styrene-ethylene-butylene-styrene (SEBS) rubber and Dodecyl benzene sulphonic acid (DBSA) doped polyaniline (PANI) composite material as a dielectric film, and carbon grease as top and bottom electrodes. From uniaxial tensile measurements, a three-dimensional constitutive model of the EAP strain sensor was validated. Experimental data obtained from the uniaxial tensile measurement was fitted according to the Ogden-based constitutive mathematical model. For predicting the stress-strain behaviour of the sensor under the multiaxial loads, 2nd term of the Ogden model was demonstrated to fit well with uniaxial tensile data. Such modelling can play a significant role in designing any type of EAP-based sensor for various operations under variable loading conditions.

Keywords: Ionic type of electroactive polymers, Strain sensors, Multiaxial loading, Constitutive modelling, Curve fitting, Uniaxial tensile testing.

1. Introduction

Electromechanical devices like actuators, sensors and generators have been widely used in robotics, healthcare, augmented reality and wearable devices [1- 5]. The last decade has witnessed a shift in the research trends from hard and brittle to soft, flexible and lightweight wearable devices. Highly elastic strain sensors that can detect large strains are highly in demand for deformable systems such as soft robotics and wearable devices. When mechanical stimuli are applied to the strain sensors then changes in capacitive and resistive values have been noticed, which makes the basis of this type of sensor technology [6-11].

Capacitive sensing has several advantages over resistive sensing like high linearity, reproducibility, and low hysteresis so currently researchers are, focusing the capacitive-based EAP sensors.

The total capacitance of EAP based capacitive sensor (C_{total}) is the sum of two capacitances, one is capacitance due to a change in its own dimension (C_1) and another is capacitance due to contact or electronic circuit, as given below:

$$C_{total} = C_1 \left(\frac{\epsilon_r \epsilon_0 A}{t} \right) + C_{parasitic},$$

where ϵ_r is the dielectric constant; ϵ_0 is the permittivity of free space; A is the active polymer area; t is the thickness of the dielectric film and $C_{parasitic}$ is the capacitance caused by contact. However parasitic capacitance is very small and can be neglected. During all types of practical applications, these EAP-based sensors undergo continuous loading and unloading conditions and multiaxial deformations.

For choosing a suitable mechanical sensor, it is very important to analyze stress-strain behaviour

under various conditions, while for elastomer-based soft sensors, it is very difficult and time-consuming to analyze the stress-strain behaviour of sensors in multi-axial loading conditions [13-14].

For designing a strain sensor for different types of loading comprehensive analytical modelling is needed, which could verify the sensor's performance experimentally. Existing papers do not provide complete modelling and neglect many crucial parameters which might affect the sensor's performance at large strain levels in the long run.

In this paper, the sensor was fabricated using Styrene-ethylene-butylene-styrene (SEBS) rubber and Dodecyl benzene sulphonic acid (DBSA) doped polyaniline (PANI) composite film (casting from the toluene solutions having 5 % concentration) sandwiched between upper and lower part with carbon grease-based electrodes. Tensile tests were performed, for analyzing the sensor's performance by using constitute equations, after post-treatment of experimental data global fitting parameters were evaluated.

These global parameters can predict sensor performance even at a large value of deformation in different types of loading. It was found that the stress-strain curve was well fit with the second order of the Ogden constitutive equation. By using fitting parameters in the Ogden model-based constitutive equation, stress can be predicted at any value of strain under multi-axial loads. This complete procedure is applicable to any type of elastomer-based capacitive strain sensor at different types of loadings.

2. Experimental

2.1. Materials

A conducting and stretchable freestanding film consisting of SEBS rubber (supplied from the Sigma-Aldrich co.) and DBSA doped polyaniline (synthesized in our laboratory at Kyutech, Japan) composite film sandwiched between carbon grease electrodes (purchased from MG chemicals) was used for fabricating Ionic type of EAP sensors. Carbon conductive tape for making the electrical connection was purchased from Nissin Co. Ltd. Our uniaxial tensile system developed at Kyushu institute of technology, Japan consisting a computer-controlled X-Y stage controller (Mark-102, Sigma Koki, Japan), load cell (LU-10 K, Kyowa), and digital Oscilloscope (TDS 2001C, Techtronic, USA).

2.2. Uniaxial Tensile Machine for Mechanical Characterization

Uniaxial tensile testing is most commonly used for characterizing the mechanical behavior of isotropic and elastic materials. Tensile measurement for the sensor used in this work was conducted using the uniaxial tensile testing system as shown in Fig. 1. It

can be seen from this figure that our tensile measurement system has a 100 N load cell, mobile stage, X-Y stage controller, and an Oscilloscope. Multiple stretching and relaxation cycles under variable strains using a stage controller and mobile X-Y stages were controlled by a computer-controlled Lab-View program. Changes in the stress under variable strain.

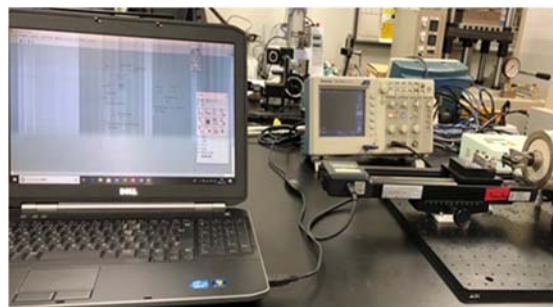


Fig. 1. Tensile measurement set-up.

2.3. Sensor Fabrication and Sample Preparation for Tensile Testing

The basic structure of the device has been shown in Fig. 2. This sensor is three layer device where DBSA doped Polyaniline SEBS rubber was used as a dielectric film and carbon grease was used as an electrode. The composite film was sandwiched between the upper and lower layer of carbon grease-based electrodes, as shown in the device structure in Fig. 2.



Fig. 2. Basic structure of stretchable carbon electrode-based ionic EAP strain sensor.

The detailed fabrication process has been described below [15]:

- Mix Polystyrene-block-poly(ethylene-ran-butylene)-block-polystyrene-graft-maleic anhydride (SEBS-g-MA) and toluene and stirred solution at 1500 rpm for 90 °C and 30 minutes at room temperature;
- After that mix DBSA-doped Polyaniline (5 %) in SEBS rubber solution;
- Then again stirred solution at 1500 rpm for 90 °C and 30 minutes at room temperature;
- Pour the solution into the desired shape of patriarch glass and heat at 90 °C for 120 minutes;
- Take dielectric film and apply carbon grease on both sides and fix carbon conducting tape on both

sides of electrodes for making the connection for measuring capacitance etc. Fig 3 shows SEBS rubber and DBSA doped polyaniline-based stretchable composite film works as a dielectric medium for ionic EAP-based sensors.

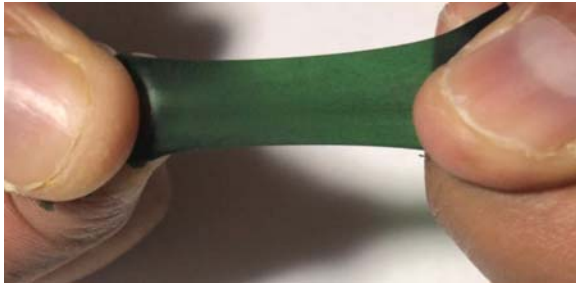


Fig. 3. DBSA doped dielectric film.

For conducting the tensile testing rectangular type of specimen having an active length of 2.8 cm, width of 1.5 mm, and thickness of 0.05 mm have been used as shown in Fig. 4. All tests were conducted at 1 mm/sec speed and fitting parameters were obtained at 100 % of strain value. Five samples were used for post-treatment of data (Among five samples, three samples were showing almost similar characteristics so one sample was chosen out of those three samples for post-treatment of data).



Fig. 4. Uniaxial tensile testing specimen.

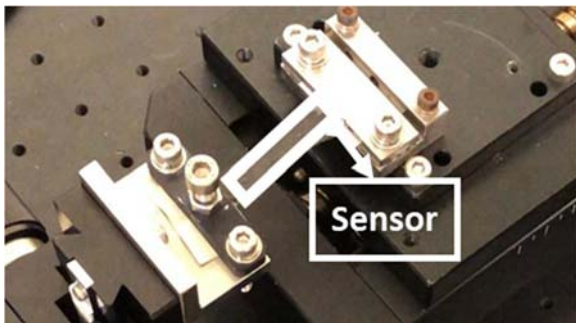


Fig. 5. Sensor fixed between two jaws of tensile machine.

Carbon grease was applied on both the upper and lower sides of the composite film and the non-conductive tape was used on both ends of the sensor for fixing the sensor between both jaws of the tensile machine. Fig .5 shows sensor is ready for uniaxial

tensile testing for analyzing the mechanical behaviour of the sensor.

3. Results and Discussion

3.1. Basic Principle of Operation

When a deformable electroactive polymer film is sandwiched between highly deformable conducting electrodes on both sides of the EAP film then the whole system works like a variable parallel plate film capacitor and its capacitance changes on applying mechanical stress, which forms the basis of such type of capacitive sensing technology [15].

The capacitance of the EAP-based strain sensor under a relaxed state ($C_{relaxed}$) can be written as:

$$C_{relaxed} = \frac{\epsilon_r \epsilon_0 L_1 L_2}{L_3}, \quad (1)$$

where, ϵ_r, ϵ_0 , are dielectric constant, the permittivity of free space, respectively and L_1, L_2, L_3 are the length, width and thickness of the sensor at relaxed state. While capacitance of EAP strain sensor in the stretched state can be written as:

$$C_{stretched} = \frac{\epsilon_r \epsilon_0 \lambda_1 \lambda_2 L_1 L_2}{\lambda_3 L_3}, \quad (2)$$

where $\lambda_1, \lambda_2, \lambda_3$ are stretch ratio in X, Y and Z direction respectively, while l_1, l_2 and l_3 are lengths, width and thickness at stretched state, consequently:

$$\lambda_1 = \frac{l_1}{L_1}, \lambda_2 = \frac{l_2}{L_2}, \lambda_3 = \frac{l_3}{L_3}$$

Here we assume EAP strain sensor shows incompressible and isotropic behavior, consequently

$$\lambda_1 \lambda_2 \lambda_3 = 1 \quad (3)$$

$$l_3 = \frac{L_3}{\lambda_1 \lambda_2} \quad (4)$$

$$C_{deformed} = C_{relaxed} (\lambda_1 \lambda_2)^2 \quad (5)$$

In case of uniaxial deformation, $\lambda_1 = \lambda$, $\lambda_2 = \frac{1}{\sqrt{\lambda}} = \lambda_3$ consequently, we can write

$$C_{stretched} = C_{relaxed} * \lambda \quad (6)$$

$$\Delta C = C_{relaxed} * \epsilon, \quad (7)$$

where ϵ is the strain, while, λ is the extension coefficient and ΔC is the change in capacitance, respectively.

In Fig. 6 we can see the schematic diagram of basic principle of operation of electroactive polymer-based strain sensors (made from the elastomeric film as a dielectric medium).

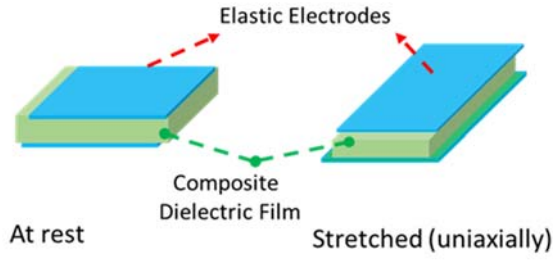


Fig. 6. Basic principle of operation of EAP -based strain sensors.

3.2. Mechanical Modelling of EAP Based Strain Sensors

The mechanical behavior of the EAP strain sensor does not follow Hook's law and nonlinear finite strain theory is used to explain EAP strain sensor behaviour as shown in Fig. 7.

Here we assumed that EAP strain sensor shows incompressible and isotropic behavior, consequently true stress T_i and strain energy potential (W) and stretch ratio λ_i can be linked by given equation [16-17].

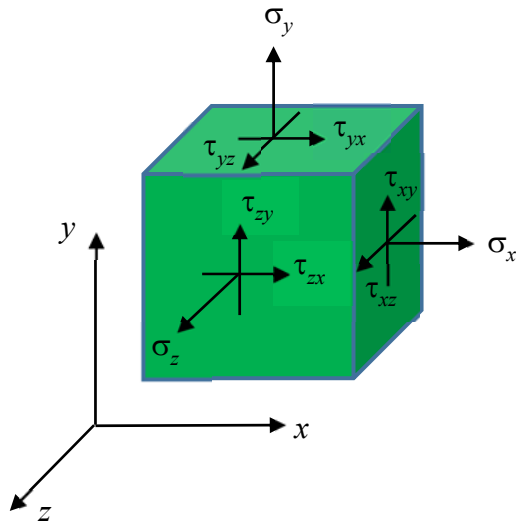


Fig. 7. Nonlinear finite strain theory for explaining EAP based strain sensor's behavior in 3D space.

$$T_i = \lambda_i \frac{\partial W}{\partial \lambda_i} - p \quad (8)$$

In above equation p is hydrostatic pressure.

Normal stress (perpendicular to a surface) can be written by equation given below:

$$\sigma_i = \frac{\partial W}{\partial \lambda_i} - \frac{1}{\lambda_i} p \quad (9)$$

The nine components of σ_{ij} can be given by the equation given as below.

$$\sigma_{ij} = \begin{pmatrix} \sigma_x & \sigma_{xy} & \sigma_{xz} \\ \sigma_{yx} & \sigma_y & \sigma_{yz} \\ \sigma_{zx} & \sigma_{zy} & \sigma_z \end{pmatrix} \quad (10)$$

Above matrix can be written as below, where off diagonal elements represent shear terms.

$$\sigma_{ij} = \begin{bmatrix} \sigma_x & \tau_{xy} & \tau_{xz} \\ \tau_{yx} & \sigma_y & \tau_{yz} \\ \tau_{zx} & \tau_{zy} & \sigma_z \end{bmatrix} \quad (11)$$

In the absence of normal shear stress τ_n (perpendicular to a surface), these three stresses perpendicular to these principal planes are called principal stresses. Fig. 8 shows the principal stresses and principal directions in 3D space.

$$\sigma_{ij} = \begin{pmatrix} \sigma_x & 0 & 0 \\ 0 & \sigma_y & 0 \\ 0 & 0 & \sigma_z \end{pmatrix} \quad (12)$$

According to the Cauchy's theorem:

$$T_i = \sigma_{ij} n_j \quad (13)$$

where T_i is the true stress vector at a point on a plane with normal vector n_i , λ is corresponded to the magnitude of normal stress vector (σ_n).

$$T_i = \lambda n_i = \sigma_{ji} n_j \quad (14)$$

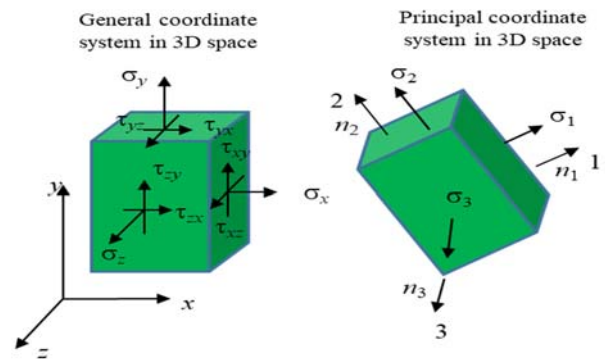


Fig. 8. Principal stresses and directions explanation using schematic diagrams.

$$\begin{aligned} (\sigma_x - \lambda)n_1 + \tau_{xy}n_2 + \tau_{xz}n_3 &= 0 \\ \tau_{xy}n_1 + (\sigma_y - \lambda)n_2 + \tau_{yz}n_3 &= 0 \\ \tau_{xz}n_1 + \tau_{yz}n_2 + (\sigma_z - \lambda)n_3 &= 0 \end{aligned} \quad (15)$$

$$\Rightarrow \begin{bmatrix} (\sigma_x - \lambda) & \tau_{xy} & \tau_{xz} \\ \tau_{xy} & (\sigma_y - \lambda) & \tau_{yz} \\ \tau_{xz} & \tau_{yz} & (\sigma_z - \lambda) \end{bmatrix} \begin{bmatrix} n_1 \\ n_2 \\ n_3 \end{bmatrix} = 0$$

$$\begin{vmatrix} (\sigma_x - \lambda) & \tau_{xy} & \tau_{xz} \\ \tau_{xy} & (\sigma_y - \lambda) & \tau_{yz} \\ \tau_{xz} & \tau_{yz} & (\sigma_z - \lambda) \end{vmatrix} = 0 \quad (16)$$

$$\Rightarrow -\lambda^3 + I_1\lambda^2 - I_2\lambda + I_3 = 0$$

This is for a homogeneous system of three linear equations, where n_i are the unknowns. Therefore, I_1 , I_2 and I_3 , called the first, second, and third stress invariants, respectively, can be given by following equations

$$I_1 = Tr|\sigma_{ij}| = \lambda_1^2 + \lambda_2^2 + \lambda_3^2 \quad (17)$$

$$I_2 = \frac{1}{2} [Tr(\sigma_{ij})^2 - Tr(\sigma_{ij}^2)] = \lambda_1^2 \lambda_2^2 + \lambda_2^2 \lambda_3^2 + \lambda_3^2 \lambda_1^2 \quad (18)$$

$$I_3 = det(\sigma_{ij}) = 1 \quad (19)$$

Different type of constitutive model for defining mechanical behavior of elastomers can be explained in terms of strain energy density (W), Invariants and coefficients as given below [18-21]:

$$W_{Mooney-Rivlin} = C_{10}(I_1 - 3) + C_{01}(I_2 - 3) \quad (20)$$

$$W_{Yeoh} = \sum_{i=1}^N C_{i0} (I_1 - 3)^i \quad (21)$$

$$W_{Neo-Hookean} = \frac{\mu}{2} (I_1 - 3) \quad (22)$$

$$W_{Ogden} = \sum_{i=1}^N \frac{\mu_i}{\alpha_i} (\lambda_1^{\alpha_i} + \lambda_2^{\alpha_i} + \lambda_3^{\alpha_i} - 3), \quad (23)$$

where λ (extension coefficient) = $1 + \epsilon$ (strain)

Table 1. Matrix representation of strain vectors and formulas for calculating invariants in various types of loading.

Loading type	Uniaxial	Pure shear	Biaxial
Strain vector	$\begin{bmatrix} \lambda & 0 & 0 \\ 0 & 1/\sqrt{\lambda} & 0 \\ 0 & 0 & 1/\sqrt{\lambda} \end{bmatrix}$	$\begin{bmatrix} \lambda & 0 & 0 \\ 0 & 1 & 0 \\ 0 & 0 & 1/\lambda \end{bmatrix}$	$\begin{bmatrix} \lambda & 0 & 0 \\ 0 & \lambda & 0 \\ 0 & 0 & 1/\lambda^2 \end{bmatrix}$
Invariants (I_1 & I_2)	$I_1 = \lambda^2 + \frac{2}{\lambda}$ $I_2 = 2\lambda + \frac{1}{\lambda^2}$	$I_1 = I_2 = 1 + \lambda^2 + \frac{1}{\lambda^2}$	$I_1 = 2\lambda^2 + \frac{1}{\lambda^4}$ $I_2 = \lambda^4 + \frac{2}{\lambda^2}$

Table 1 shows the matrix representation of strain vectors for different kind of loads and equations for calculating invariants at different kind of loading conditions. With the help of Table 1 we can easily calculate the strain energy density for different kind of constitutive equations, as explained above (from equation 20 to 24) and further we can also establish relationship between stress and strain for any kind of constitutive equation by using equation 9.

3.3. Mechanical Characterization of EAP Strain Sensor

Force displacement characteristics as shown in Fig. 9, we can conclude that sensor shows purely elastic behavior as cycles are repetitive, following same trend and stress is almost constant in each cycle.

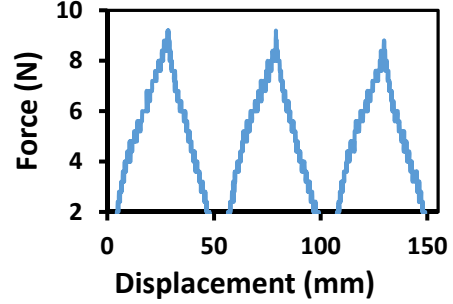


Fig. 9. Force displacement characteristics of Ionic EAP based strain sensor.

From Fig. 10 we can see that sensor is highly stretchable and can be elongated more than 400 % of strain value.

For elongation at break test sample's length, width, thickness was 2 cm, 1 cm, 0.2mm respectively.

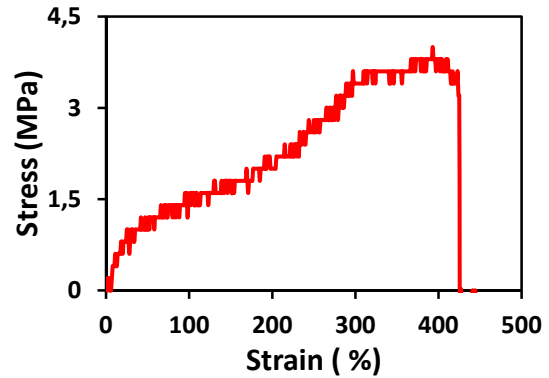


Fig. 10. Elongation at break test of EAP strain sensor.

3.4. Predicting Stress Strain behavior of EAP Strain Sensor under Multiaxial Loads

First stretching cycle up to 100 % applied strain was used for the mechanical modelling using Ogden based constitutive model and it can be seen from the Fig. 11 that there was good agreement between the experimental data and fitting of the data using the Ogden 2nd terms constitutive equation (in stress versus strain form). Fitting parameters (less than 10 % deviation for 5 samples) are summarized in the Table 2. For curve fitting cftool (in Matlab), hyperfit or abaqus can be used. Here curve fitting was done using Hyperfit software <http://www.hyperfit.wz.cz> (Ansys-compatible original form).

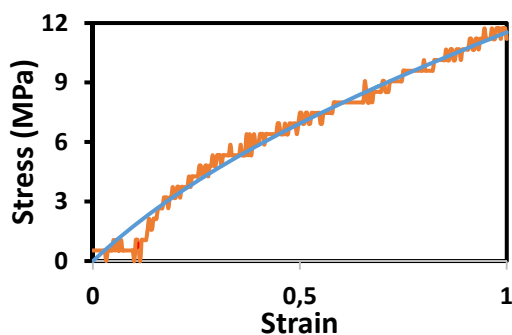


Fig. 11. Fitting of experimental data with Ogden Modelling for ionic type of EAP strain sensor.

Table 2. Ogden fitting parameters.

Fitting parameters	Ogden 2 nd order
μ (MPa)	6.51, -0.02
α (MPa)	2.02, 3.18

With the help of fitting parameters, we can predict the stress-strain behavior (uniaxial loading) of the sensor at any value of strain by using equation 23, Table 1 and section 3.2 (as shown in figure Fig. 11 and Table 2). Similarly, we can also use these fitting parameters in predicting stress in biaxial and planar loading as well.

4. Conclusions

Sensor was highly stretchable and can be stretched up to 400 % of strain value. From uniaxial tensile experiments, a three-dimensional constitutive model of the EAP strain sensor was validated. Sensor was showing good agreement with Ogden's 2nd terms and these fitting parameters obtained from uniaxial tensile data can also be used for predicting sensor's behavior under multiaxial loading. This type of analytical modelling can be useful in designing elastomer-based strain sensor for various loading conditions.

Acknowledgement

One of the authors **Nitin Kumar Singh** would like to thank ministry of education, culture, sports and Science (MEXT), Japan for providing the scholarship.


References

- [1]. N. K. Singh, K. Takashima, and S. S. Pandey, Tear strength estimation of electroactive polymer-based strain sensors, in *Electroactive Polymer Actuators and Devices (EAPAD) XXIV*, J. D. Madden, I. A. Anderson, and H. R. Shea, Long Beach, United States, Mar. 6–Apr. 11, 2022. SPIE, 2022.
- [2]. N. K. Singh, K. Takashima, and T. Shibata, Dielectric elastomer based stretchable textile sensor for capturing motion, in *Electroactive Polymer Actuators and Devices (EAPAD) XXII*, Y. Bar-Cohen, I. A. Anderson, and H. R. Shea, Eds. Online Only, United States, Apr. 27–May 8, 2020. SPIE, 2020.
- [3]. X. Liu et al., Dielectric elastomer sensor with high dielectric constant and capacitive strain sensing properties by designing polar-nonpolar fluorosilicone multiblock copolymers and introducing poly(dopamine) modified CNTs, *Composites Part B: Engineering*, Vol. 223, 2021, p. 109103.
- [4]. N. K. Singh, K. Takashima, and S. S. Pandey, Electronic versus Ionic Electroactive Polymers (EAPs) Strain Sensors for Wearable Electronics: A Comparative Study, *Eng. Proc.*, 21, 1, 2022.
- [5]. N. K. Singh, K. Takashima, and S. S. Pandey, Fatigue life prediction of electroactive polymer strain sensor, *Proceedings Volume 11587, Electroactive Polymer Actuators and Devices (EAPAD) XXIII*, 2021, 115871Z.
- [6]. N. K. Singh, K. Patra., A. Kumar, Energy harvesting using Dielectric Elastomer, in *Proceedings of the International Conference on Advanced Materials for Power Engineering (ICAMPE-2015, Kerala, India)*, 2015.
- [7]. P. C. Binh, D. N. C. Nam, K. K. Ahn, Modeling and experimental investigation on dielectric electro-active polymer generator, *International Journal of Precision Engineering and Manufacturing*, Vol. 16, No. 5, May 2005, pp. 945–955.
- [8]. N. K. Singh., K. Patra, Energy harvesting using dielectric elastomer, Master thesis, *Indian Institute of Technology Patna*, India, 2014.
- [9]. K. Ozlem, O. Atalay, A. Atalay, and G. Ince, Textile based sensing system for lower limb motion monitoring, in *Converging Clinical and Engineering Research on Neurorehabilitation III*, Springer International Publishing, Cham, 2018, pp. 395–399.
- [10]. Y.-D. Tao, G.-Y. Gu, and L.-M. Zhu, Design and performance testing of a dielectric elastomer strain sensor, *International Journal of Intelligent Robotics and Applications*, Vol. 1, No. 4, 2017, pp. 451–458.
- [11]. J.-W. Zhang, Y. Zhang, Y.-Y. Li, and P. Wang, Textile-Based flexible pressure sensors: A review, *Polymer Reviews*, 2021, pp. 1–31.
- [12]. K. Jung, K. J. Kim, and H. R. Choi, A self-sensing dielectric elastomer actuator, *Sensors and Actuators A: Physical*, Vol. 143, No. 2, 2008, pp. 343–351.
- [13]. N. K. Singh, K. Takashima, and S. S. Pandey, Electrical characterization and analytical modeling for predicting stress-strain behavior of electroactive polymer-based sensors under multiaxial loads, in *Proceedings of the 8th International Conference on Sensors and Electronic Instrumentation Advances (SEIA' 2022)*, Corfu, Greece, 21–23 September 2022, pp. 28–30 (accepted in June 2022).
- [14]. A Qiu, Q Jia, H Yu, J. A. Oh, D Li, H. Y. Hsu, and J. Ma, Highly sensitive and flexible capacitive elastomeric sensors for compressive strain measurements, *Materials Today Communications*, 26, 2021, 102023.
- [15]. N. Ni and L. Zhang, Dielectric Elastomer Sensors, in *Elastomers*, *InTech*, 2017.
- [16]. X. Chen, N. Laforge, Q. Ji, H. Tan, J. liang, Introduction to mechanical metamaterials and their effective properties, *Comptes Rendus. Physique*, November 2020, pp. 1–15.

- [17]. Z. Suo, Theory of dielectric elastomers, *Acta Mechanica Sinica*, Vol. 23, No. 6, 2010, pp. 549–578.
- [18]. Y. Bai, C. Liu, G. Huang, W. Li, and S. Feng, "A Hyper-Viscoelastic Constitutive Model for Polyurea under Uniaxial Compressive Loading," *Polymers*, vol. 8, no. 4, p. 133, April 2016.
- [19]. S. D. Barforooshi and A. K. Mohammadi, Study Neo-Hookean and Yeoh Hyper-Elastic Models in Dielectric Elastomer-Based Micro-Beam Resonators, *Latin American Journal of Solids and Structures*, Vol. 13, No. 10, 2016, pp. 1823–1837.
- [20]. A. A. Abdelsalam, S. Araby, M. A. Hassan, and A. A. El-Moneim, "Constitutive modelling of elastomer/graphene platelet nanocomposites," *IOP Conference Series: Materials Science and Engineering*, Vol. 244, p. 012016, September 2017.
- [21]. R. W. Ogden (1972). Large deformation isotropic elasticity—on the correlation of theory and experiment for incompressible rubberlike solids. *Proceedings of the Royal Society of London. A. Mathematical and Physical Sciences*, 326 (1567), pp. 565-584.

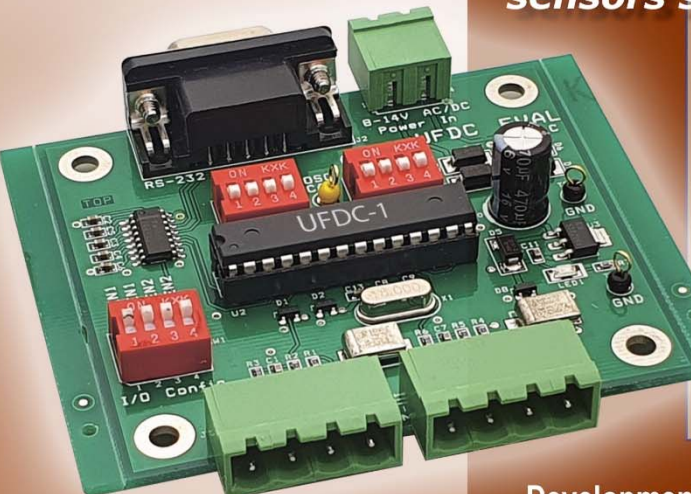


Published by International Frequency Sensor Association (IFSA) Publishing, S. L., 2022 (<http://www.sensorsportal.com>).



Easy and quick

sensors systems development



Development Board UFDC-1/UFDC-1M-16

- 16 measuring modes, 2 channels for frequency measurements
- Frequency range from 0.05 Hz up to 7.5 MHz (120 MHz)
- Programmable accuracy from 1 % up to 0.001 %
- RS232 (USB optional)

sales@sensorsportal.com
http://www.sensorsportal.com/HTML/E-SHOP/PRODUCTS_4/Evaluation_board.htm

